Heat transfer model for cw laser material processing

Cite as: Journal of Applied Physics **51**, 941 (1980); https://doi.org/10.1063/1.327672
Published Online: 09 July 2008

J. Mazumder, and W. M. Steen

Heat transfer model for cw laser material processing

J. Mazumder and W.M. Steen
Department of Metallurgy and Materials Science, Imperial College of Science and Technology, London SW7 2BP, England

(Received 19 September 1979; accepted for publication 12 October 1979)

A three-dimensional heat transfer model for laser material processing with a moving Gaussian heat source is developed using finite difference numerical techniques. In order to develop the model, the process is physically defined as follows: A laser beam, having a defined power distribution, strikes the surface of an opaque substrate of infinite length but finite width and depth moving with a uniform velocity in the positive x direction (along the length). The incident radiation is partly reflected and partly absorbed according to the value of the reflectivity. The reflectivity is considered to be zero at any surface point where the temperature exceeds the boiling point. This is because a "keyhole" is considered to have formed which will act as a black body. Some of the absorbed energy is lost by reradiation and convection from both the upper and lower surfaces while the rest is conducted into the substrate. That part of the incident radiant power which falls on a keyhole is considered to pass into the keyhole losing some power by absorption and reflection from the plasma within the keyhole as described by a Beer Lambert absorption coefficient. Matrix points within the keyhole are considered as part of the solid conduction network, but operating at fictitiously high temperatures. The convective heat transfer coefficient is enhanced to allow for a concentric gas jet on the upper surface as used for shielding in welding and surface treatment, but not cutting. The system is considered to be in a quasi-steady-state condition in that the thermal profile is considered steady relative to the position of the laser beam. The advantages of this method of calculation over others are discussed together with comparisons between the model predictions and experiments in laser welding, laser arc augmented welding, laser surface treatment, and laser glazing. The system is assumed to be in a quasi-steady-state condition after the keyhole initiation period which for most practical purposes may be considered instantaneous.

PACS numbers: 44.10. + i, 44.40. + a

I. INTRODUCTION

The laser is finding increasing commercial use as a welding,[1-4] cutting,[2,5] or surface treatment[5-8] tool. However, for its use to be consolidated it is necessary to understand how it works in these processes and to predict how it would work in novel situations or on novel materials.

In understanding how it works the experimenter is faced with a multiparameter problem which is difficult to solve without extensive factorial experimentation. The principal variables are the substrate thermal and optical properties, the laser beam's total power, power distribution and diameter, and the traverse speed. Alternatively, as described here, an assumed physical picture of the process can be modelled mathematically and the model's results compared to experimental results to prove the model's validity and thus by inference the physical model.

A model capable of predicting experimental results means that previously unmeasurably parameters can be estimated. In metal welding Borland and Jordan[9] summarized the most important data to be (1) the thermal cycle at each location in the fusion and heat affected zone (HAZ), which defines the extent of any phase change, (2) the peak temperature distribution, and (3) the cooling rates which would affect the formation of metastable structures such as martensite. Without a mathematical model the values of these parameters are very difficult to obtain.

Further a model is capable of checking the mythology that grows around any process. For example, how important is the surface reflectivity in laser welding, cutting, or surface hardening? Or would there be back tempering if traces are overlaid while surface hardening?

Since a mathematical model gives these advantages of checking a physical model, estimating important parameters, and calculating the effect of varying any parameter, it is not surprising that many workers have built them. A useful review of theoretical techniques which have been used in welding has been written by Myers, Uyehara, and Borman.[10] Perhaps the best known in the welding field is the analytic solution for a moving point source on thick and thin sheets which was developed by Rosenthal[11,12] in 1941. Since this model does not allow for "keyholing", its results are almost irrelevant to laser processing and indeed its predictions of fusion zones can be out by a whole order.

To allow for the keyhole effect whereby the intense energy of the laser vaporizes a fine hole into the substrate, Swifthook and Gick[13] built an analytical model based on a line source through the substrate. This gives a better prediction but by definition is unable to calculate depths of penetration.

A summary of some of the relevant analytic solutions is given in Table I.

A numerical solution is needed if the nonlinear terms of surface reradiation and keyholing are to be included.

A stationary heat source model was developed by Steen[14] for vapor deposition studies using a laser.[7] Moving

 0021-8979/80/020941-07$01.10

TABLE I. Summary of analytic solutions to the spot heating problem.

Type of mathematical model	Particular Process aimed	Reference
Moving point heat source for three-dimensional heat flow	General welding processes	9, 11, 12, 37
Moving line heat source for two-dimensional heat flow	General welding processes	9, 11, 12, 37
Moving line source for two-dimensional heat flow	Laser and electron beam	13
Uniform and finite heat source for one-dimensional heat flow	CO_2 laser welding	38 38
Uniform band or rectangular heat source for steady-state two-dimensional heat flow	EBW and cw laser welding	39
Uniform circular heat source of a semifinite slab (i.e., for two-dimensional heat flow calculating transient surface isotherms)	Pulsed laser	40
Stationary Gaussian or uniform circular heat source for transient temperature distribution in thin film	Electron beam heating	41
Moving cylindrical source	Thermic cutting electron beam cw laser	42

source solutions mainly directed towards the welding process have been made by Rykalin,[15,16] Westby,[17] Arata and Inoue,[18] and Paley and Hibbert.[19] Westby's model[17] allowed for heat flow in one or two dimensions in a substrate having variable thermal properties. Arata and Inoue[18] developed a solution for a moving line source having a nonuniform input along its length. The aim was to more accurately model the temperature in the vicinity of the heat source. Paley and Hibbert[19] developed Westby's model so that it could simulate double V and U grooves and have heat flow in three dimensions.

Attempts have been made to model the highly complex keyhole region of a laser surface interaction. The semiquantitative calculation of Klemens[20] proved remarkably successful even though he assumed only one-dimensional flow along the quadrant position around the keyhole.

In this paper a numerical model is described which is capable of calculating the necessary metallurgical data as well as the depth of penetration. The model allows for surface heat losses on the upper and lower surfaces of a slab of finite thickness and width but infinite length, and also allows for the formation of a keyhole. It does not allow for variable thermal properties, latent heat effects, or chemical reaction within the substrate, nor is a heat balance on the laser generated plasma within the keyhole attempted.

II. DERIVATION OF A MATHEMATICAL MODEL

A. Physical definition of the process to be modelled

In order to develop the mathematical model the process is physically defined as follows:

A laser beam having a defined power distribution strikes the surface of an opaque substrate having finite width and thickness and infinite length moving in the positive x direction (along the length) with a uniform velocity. Some of the incident radiation is reflected. The rest is absorbed, but the reflectivity is considered to be zero if the temperature exceeds the boiling point since it is then assumed that a keyhole is produced by vaporization which acts as a blackbody. Some of the absorbed energy is lost by radiation and convection from the surface while the rest is conducted into the substrate. The convective heat transfer is enhanced on the upper surface due to a concentric gas jet used for shielding.

The three-dimensional system is assumed to be in a quasi-steady-state condition after the keyhole initiation period, which for most practical purposes may be regarded as instantaneous[21] and will only occur at the beginning of a welding run.

This leads to the following assumptions:

(1) The laser beam remains stationary relative to earth and is incident at right angles at the center of the substrate width. The substrate moves in the positive x direction (along the length) with uniform velocity U. The system is diagrammatically shown in Fig. 1.

(2) The workpiece is infinite in length (i.e., in the x direction) but has finite width and thickness.

(3) Quasi-steady-state is assumed.

(4) The power distribution in the beam is Gaussian (not a necessary assumption, but a precise distribution is required and a Gaussian distribution approximates that from a well-tuned laser with a stable cavity).

(5) The thermal conductivity, density, and specific heat are independent of temperature.

(6) Latent heat of fusion is compensated by latent heat of solidification (this would have the effect of shortening the downstream isotherms).

(7) Reflectivity is considered to be zero when the temperature exceeds the boiling point.

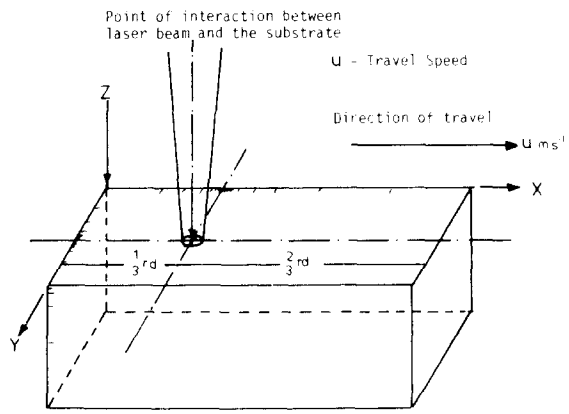

FIG. 1. Geometry of the total calculation volume with respect to the laser beam.

(8) There is a radiation loss from the upper and lower surfaces of the workpiece.

(9) There is a convective heat loss due to shielding gas flow.

(10) When any location exceeds the boiling point it is considered to have evaporated.

(11) Radiation penetrating the substrate is absorbed according to Beer Lambert's law,

$$P = P_s e^{-\beta L}, \tag{1}$$

where β is the absorption coefficient m^{-1} and is considered independent of position within the keyhole, and P is the radiant power at depth L which was of value P_s at the surface.

(12) Matrix points considered to have "evaporated" remain in the conducting network at a fictitiously high temperature to simulate the high convection and radiation transfer effects from the fast moving plasma within the keyhole.

B. Mathematical definition of the process to be modelled

1. Method of solution

A large number of numerical techniques have been reported to solve partial differential equations.[22-28] Since the present problem concerns a given steady-state situation, a "relaxation" technique was chosen.[29]

For computing stability it was found that at least five grid points must lie within the incident laser beam diameter. Since this diameter is approximately 250 μm, the only way the program could fit a computer with a finite store and yet model a slab of reasonable size was to have an exponentially expanding grid.[29]

The heat balance on an asymmetric control volume within the body of the exponential grid, as shown in Fig. 2, can be stated in Cartesian coordinates as

$$-K\delta y\delta z\left(\frac{\partial T}{\partial x}\right)_{PW} - K\delta x\delta z\left(\frac{\partial T}{\partial y}\right)_{PN} - K\delta x\delta y\left(\frac{\partial T}{\partial z}\right)_{PH} + K\,\delta y\,\delta z\left(\frac{\partial T}{\partial x}\right)_{EP} + K\,\delta x\,\delta z\left(\frac{\partial T}{\partial y}\right)_{SP} - K\,\delta x\,\delta y\left(\frac{\partial T}{\partial z}\right)_{LP} + \rho\mu\, C\rho\,\delta y\,\delta z\left(\frac{T_W + T_P}{2}\right) - \rho\mu\, C\rho\,\delta y\,\delta z\left(\frac{T_P + T_E}{2}\right) = 0, \tag{2}$$

where K = thermal conductivity $Wm^{-1}\,K^{-1}$, subscripts P, E, W, S, N, H, and L refer to the locations shown in Fig. 2 for the temperature T.

Thus for a location within the body of the substrate the finite difference equations become after dividing by $(\rho\, C\rho\,\delta x\,\delta y\,\delta z)$,

$$-\frac{2\alpha}{(X_E - X_W)}\left(\frac{T_P - T_W}{X_P - X_W}\right) - \frac{2\alpha}{(Y_S - Y_N)}\left(\frac{T_p - T_N}{Y_p - Y_N}\right) - \frac{2\alpha}{(Z_L - Z_H)}\left(\frac{T_P - T_H}{Z_P - Z_H}\right) + \frac{2u}{(X_E - X_W)}\left(\frac{T_P + T_W}{2}\right) + \frac{2\alpha}{(X_E - X_W)}\left(\frac{T_E - T_P}{X_E - X_P}\right) + \frac{2\alpha}{(Y_S - Y_N)}\left(\frac{T_S - T_P}{Y_S - Y_P}\right) + \frac{2\alpha}{(Z_L - Z_H)}\left(\frac{T_L - T_P}{Z_L - Z_P}\right) \times \frac{2u}{(X_E - X_W)} - \left(\frac{T_E + T_P}{2}\right) = 0, \tag{3}$$

where α = thermal diffusivity m^2/s. Equation (3) was used to solve all grid points. At the surface or edge locations where one of the temperature gradients becomes ambiguous special values of the gradients were calculated.

Thus for surface points

$$K\left(\frac{\partial T}{\partial x}\right)_{x,y,1} = P_{x,y}(1 - r_f) - (h_c + h_r)(T_{\underset{x,y}{\text{surf}}} - Ta), \tag{4}$$

where Ta = ambient temperature °K and $T_{\underset{x,y}{\text{surf}}}$ = surface temperature of substrate at position x, y, from which derives the term

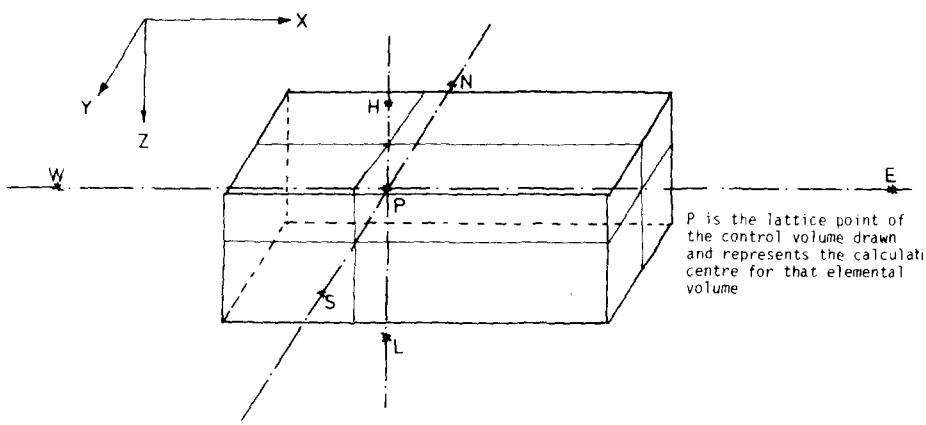

FIG. 2. Nomenclature used in and around an elemental control volume.

$$\frac{2\alpha}{(Z_L - Z_H)}\left(\frac{T_P - T_H}{Z_P - Z_H}\right) = \frac{\alpha}{(Z_L - Z_{\text{surf}})}\frac{\left|P_{x,y}(1 - r_f) - (h_c + h_f)(T_{\text{surf}} - Ta)\right|_{x,y}}{k}, \tag{5}$$

which is substituted into Eq. (3).

The value of $P_{x,y}$ for a TEM_{00} mode structure is that given by a Gaussian power distribution such that

$$P_{x,y} = \frac{P_{\text{tot}}}{r_b^2 \pi} \exp\left(-\frac{2r}{r_b^2}\right), \tag{6}$$

where $r = (x^2 + y^2)^{1/2}$ is the radial distance from the center m, P_{tot} is the total incident power in the laser beam W, and r_b is the Gaussian beam radius defined as the radial distance at which the power density falls to $1/e^2$ the central value m.

The convective heat transfer coefficient h_c required in Eq. (5) is calculated from Gordon and Cobonpue[30] for the case of a vertically impinging jet

$$h_c = 13 Re^{0.5} Pr^{0.33} k_{\text{gas}}/B, \tag{7}$$

where B is the jet plate distance, Re is the Reynolds number at jet exit, Pr is the Prandtl number for the gas, and k is the thermal conductivity of the gas.

Variation of h_c with radial location was ignored due to the relatively small contribution of the convective term. It could have been allowed for as described by Davies.[31]

The radiative heat transfer coefficient h_r is derived from its definition

$$q_{r\,\text{loss}} = h_{r_{x,y}} A (T_{\text{surf}_{x,y,1}} - Ta), \tag{8}$$

and the Stefan-Boltzmann equation

$$q_{r\,\text{loss}} = A\sigma(1 - r_{f_{x,y}})(T^4_{\text{surf}_{x,y,1}} - Ta^4), \tag{9}$$

from which derives

$$h_{r_{x,y}} = \sigma(1 - r_{f_{x,y}})(T^2_{\text{surf}_{x,y,1}} + Ta^2)(T_{\text{surf}_{x,y}} + Ta). \tag{10}$$

The keyholing simulation[29,32] was achieved by calculating $T^{\text{surf}}_{x,y}$ for surface grid points and if it exceeded the boiling point of the material, then that grid point was deemed to be transparent and the incident power fell on the grid point below it after suffering some absorption and so on through the substrate while the transparent grid points kept their high temperature (as would be the case if the keyhole were filled with hot plasma).

The absorption of the radiation penetrating the substrate was considered to be independent of depth or lateral position, i.e., no account was taken of temperature variation within the plasma filled keyhole. Thus the power entering the keyhole $P_{x,y}$ became

$$P'_{xy} = P_{xy} e^{-\beta L},$$

where β is absorption coefficient m^{-1} after penetrating a depth L into the plasma filled keyhole.

The range of reasonable values for the absorption coefficient β was calculated by considering that if a material (e.g., mild steel) has a typical surface reflectivity to 10.6 μm radiation of 80%, the remaining 20% of incident power from the laser is sufficient to initiate a keyhole, at which point the keyhole behaves as a black body and absrobs 100% of the power. Absorption takes place in the plasma filled keyhole due to the high electron density of the hot vapor (~20 000 °K). Now it has been observed by many workers, e.g., Alexander[33] that the laser penetration at 1300 W into mild steel achieves a depth of 2.3 mm virtually independent of speed over the range 5–25.0 mm/s;at 1500 W the depth is 2.5 mm; at 1700 W it is 2.72 mm. From these figures it is straightforward to calculate via Eq. (1) that only above an absorption coefficient of 700 m^{-1} is less than 20% of the beam power available at the maximum penetration depth, i.e., less than the power required to initiate the keyhole. (It is interesting to note that these depths all give the same residual power available at the limiting depth for the same assumed absorption coefficient.) Thus a value of 800 m^{-1} was chosen as a reasonable value for the absorption coefficient when welding mild steel—a value in line with that used by others.[20]

The bottom surface, similar to the top surface, had a specially calculated z gradient,

$$\left(\frac{\partial T}{\partial z}\right)_{z,y,1Z} = -(h_c + h_r)(T_{\text{surf}} - Ta)/k. \tag{11}$$

The boundary edges, which were arranged to be well away from the laser event, had their edge gradients calculated by assuming the next grid point beyond the analysis zone was at the ambient temperature (Ta).

The overall matrix size ($32 \times 31 \times 4$) was decided by the available core storage (CDC 6500 + CYBER 174 with central memory of 227 k, 60 bit words). The grid spacing was decided by stability and computing time considerations.

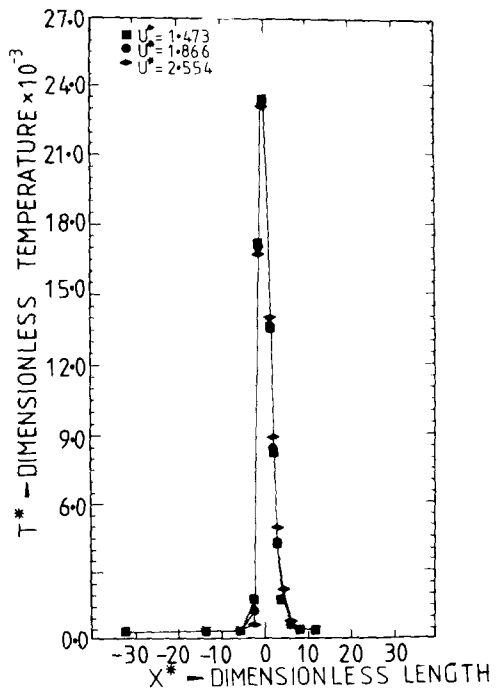

FIG. 3. Center line T^* versus X^*.

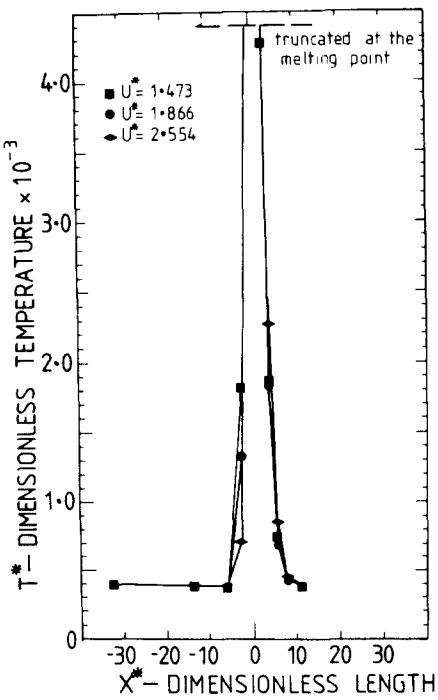

FIG. 4. Center line T^* versus X^* larger scale and truncated.

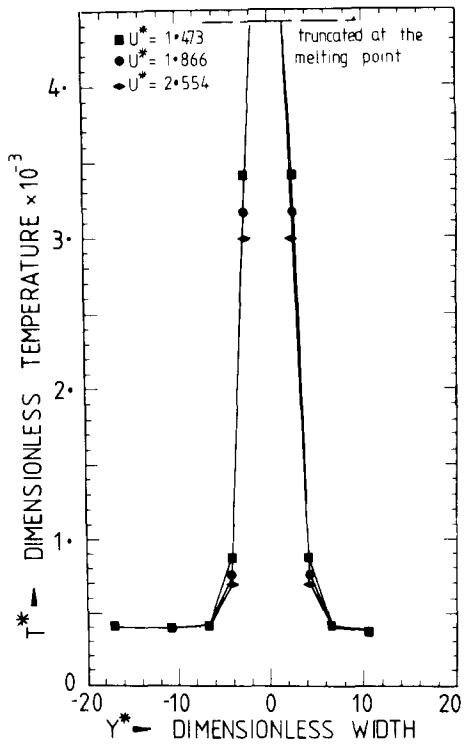

FIG. 6. T^* versus Y^* with larger scale.

The accuracy of the answer was checked by showing that it was independent of computation parameters such as grid spacing and convergency limits and that the answer agreed with experimental runs.

Considerable saving in computing time was achieved by introducing a weighting factor (over relaxation) for resetting temperatures which was a function of the largest temperature change made in the previous iteration cycle such that

$$T_1' = T_1 + R/[W\exp(-\Delta T_{\max}/\gamma)],$$

where T_1' is the new value of T_1, R is the residual at that grid point, W is a constant, $\Delta T_{\max}$ is the largest change in temperature calculated on that iteration cycle, and γ is a variable weighting factor dependent on the value of ΔT.

A further saving in computation time was obtained by

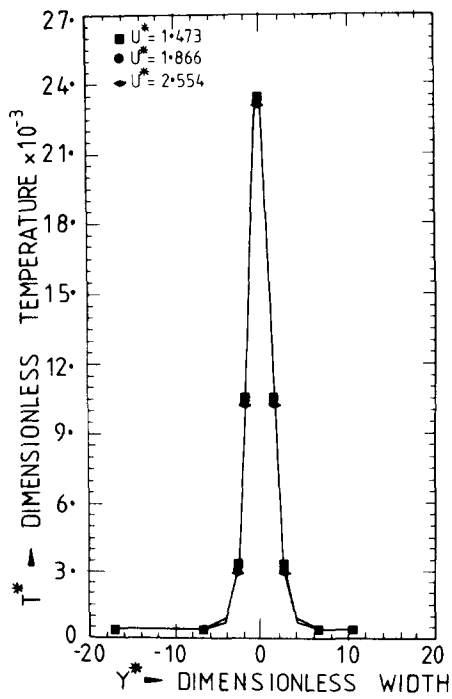

FIG. 5. T^* versus Y^* through the point of intereaction.

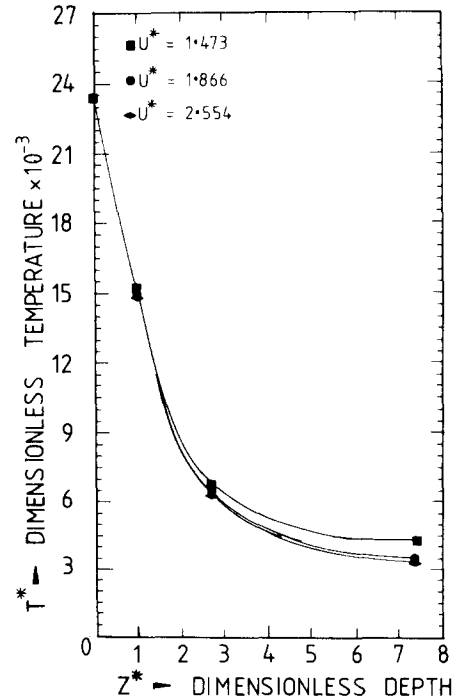

FIG. 7. T^* versus Z^* through the point of interaction.

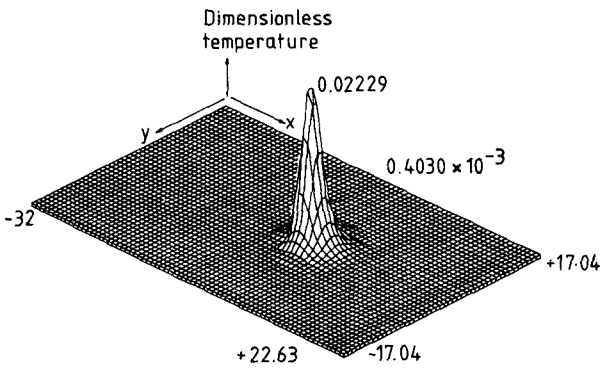

FIG. 8. Dimensionless surface temperature distribution.

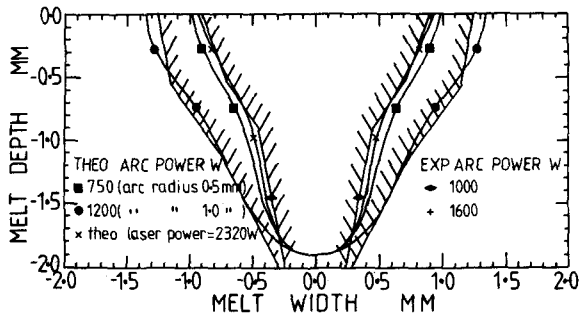

FIG. 10. A comparison of the predicted and experimental fusion zones associated with the 1.0 and 1.6 kW laser/arc welding runs. The theoretical arc power transferred = 75%, laser incident power = 1.57 kW, welding velocity 33.5 mm/s, and absorption coefficient = 800 m^{-1}.

introducing an adiabatic boundary along the central axis of symmetry running in the *xz* plane and performing the calculation on only one-half of the imaginary slab.

III. OPERATION OF THE MODEL

The mathematical model could be used for the following purposes: (1) to predict the temeprature profile, (2) to predict maximum welding speeds, (3) to predict the heat affected zone, (4) to predict the thermal cycle at any location or speed, (5) to predict the effect of thickness or any other parameter (e.g., reflectivity, thermal conductivity, etc.), or (6) to predict the effect of supplementary heating or cooling.

The results from the model can either be represented in real units to simulate a particular run or shown as generalized curves using dimensionless groups. The groups identified as of principal importance were

$$T^* = \frac{\Delta T k D_b}{P_{\text{tot}}(1 - r_f)},$$

$$X^* = \frac{X}{D_b},$$

$$Y^* = \frac{y}{D_b},$$

$$Z^* = \frac{z}{D_b},$$

$$U^* = \frac{UD_b}{\alpha},$$

where D_b is the incident beam diameter defined as in Eq. (6). These variables are plotted in Fig. 3–8. The advantage of generalized plots is that a reasonable prediction for the temperature profile may be obtained for different operating conditions without further recourse to the computer. But due to there being too many variables involved it is difficult to represent the effect of all the variables in one single plot.

The temperature profiles calculated can be used to predict the extent of metallurgical changes. Some results compared to experiments are discussed below.

(a) *Surface hardening.* Steen and Courtney[6] in their work on laser heat treatment of EN8 steel found that predicted width and depth of heat affected zone by the model correlates reasonably well with their experimental observations.

(b) *Laser glazing.* The prediction for the width and depth of the laser skin melted zones of nickel alloy (Mar-M002) were compared with the experimental observations and found to be reasonably accurate.[34] For example, the depth of penetration for coated Mar-M002 at 1730 W and 366 mm/s was predicted to be 0.2 mm, whereas experimental observations found it to be 0.18 mm and there was also a correlation between fusion and heat affected zone profiles.

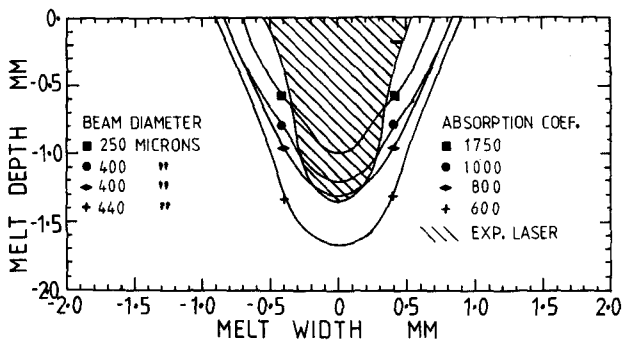

FIG. 9. Variation in laser melt widths with beam diameter and absorption coefficient at a laser power of 1570 W and reflectivity of 0.8. Welding velocity 33.5 mm/s.

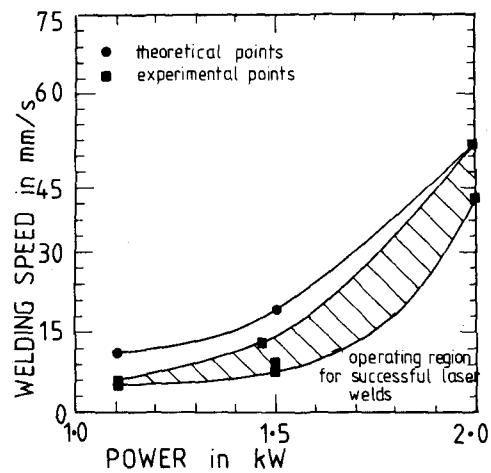

FIG. 11. Mathematically predicted cooling rate for Ti weld (6A 1-4 V); 1500 W, 7.5 mm/s, 2 mm thick.

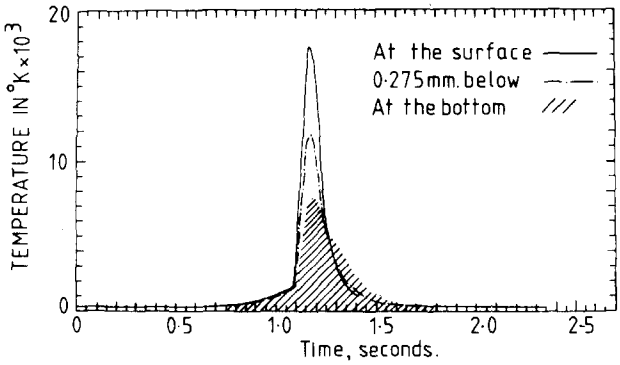

FIG. 12. Comparison of model predictions and experiment showing the variation of the welding speed for 2-mm titanium (6A 1–4 V) with laser incident power.

(c) *Welding.* Predictions of the fusion zone have been successfully made for Ti welds[29,35] and welds in mild steel.[32,36] The comparison of predicted and experimental fusion zones for a partial penetration bead-on-plate weld in mild steel is shown in Fig. 9, which also shows the effect of varying the absorption coefficient—note the beam diameter is not constant in the figure. Using an electric arc and a laser heat source together[32,36]—the arc having an assumed parabolic power distribution—a fit with the observed fusion zones and a comparison with the expected fusion zone from a more powerful laser is shown in Fig. 10. By resetting the traverse speed during the relaxation iteration, the maximum speed at which the melting point is just achieved on the lower surface can be calculated. This would be expected to be similar to or slightly higher than the maximum welding speed. It compares well with experiments in the welding of 2-mm Ti (Fig. 11).

It is also possible to calculate the thermal cycle experienced by titanium under these welding conditions (Fig. 12). This datum is almost impossible to measure. However, the cooling rate has a marked effect on the resulting microstructure and is thus worth knowing.

Further it is also possible to integrate the thermal fluxes through different zones and so find the overall utilization of energy within the welding system. For example, welding at 1500 W and 7.5 mm/s and considering only a 10-cm length of weld, heat in slab is 245 W; heat reradiated is 1175 W; heat convected and reflected is 80 W. Finally, by comparing experiments and calculations a quantitative estimate of the rate of grain growth or diffusion can be made. This study is currently in hand.

IV. CONCLUSION

It is possible by the numerical technique illustrated here to predict the fusion, the heat affected zone, and thermal cycles in the neighborhood of a laser/surface interaction; and from these figures to calculate the conditions such as the maximum welding speed as a function of laser power, or substrate thickness.

[1]R.C. Crafer, Welding Inst. Conf. and 4th Int. Conf., Harrogate, 9–11 May 1978, paper 46, pp. 267–271.
[2]J.D. Russel, Welding Inst. Res. Bull., pp. 345–350, December 1975.
[3]C.M. Banas, CEGB Conf. 17–21 Sept. 1972, paper 41, pp. 565–573.
[4]A.B.J. Sullivan and P.T. Houldcroft, Brit. Weld. J. **14**, 443 (1967).
[5]W.W. Duley, *CO_2 Lasers, Effects and Applications* (Academic, New York, 1976).
[6]C. Courtney and W.M. Steen, Metal Technology pp. 456–462, Dec. (1979).
[7]W.M. Steen, paper 3, Int. Conf. Welding Inst., London, Feb. 1978.
[8]C. Courtney and W.M. Steen, Laser '79 Conference, Munich, 1979.
[9]J.C. Borland and H.F. Jordan, Inst. of Metallurgists Review Course, series 2, no. 9, p. 95, Oct. 1972.
[10]P.S. Myers, O.A. Uyehara, and G.L. Borman, Weld. Res. Council Bull. **123**, pp. 1–46 (1967).
[11]D. Rosenthal, Welding J. **20**, 2205S–2255S (1941).
[12]D. Rosenthal, Trans. ASME **48**, 848–866 (1946).
[13]D.T. Swifthook and A.E.F. Gick, Welding J. **52**, 492S–499S (1973).
[14]W.M. Steen, Lett. Heat Mass Transf. **4**, 167–178 (1977).
[15]N.N. Rykalin, (unpublished).
[16]N.N. Rykalin, *The Calculation of Thermal Processes in Welding Mashgiz* (1951). Translated into English by Z. Paley and C.M. Adams Jr. (1963).
[17]Ola Westby, The Technical University of Norway (1968) (unpublished).
[18]Y. Arata and K. Inoue, Trans. JWRI **2**, 41–45 (1973).
[19]Z. Paley and P.D. Hibbert, Welding J. **54**, 385S–392S (1975).
[20]P.G. Klemens, J. Appl. Phys. **47**, 2165–2174 (1976).
[21]R.C. Crafer, Welding Inst. Res. Bull. **17**, pp. 28–33 (1976).
[22]V.S. Dorn and D.D. McCraken, *Numerical Methods and Fortran Programming* (Wiley, New York, 1964).
[23]G.M. Dusinberre, *Numerical analysis of Heat Flow* (McGraw-Hill, New York, 1949).
[24]J.B. Scarborough, *Numerical Mathematical Analysis*, 6th ed. (John Hopkins Press, Baltimore, 1966).
[25]G. Leibmann, Brit. J. Appl. Phys. **6**, 129 (1955).
[26]J. Crank and P. Nicholson, Proc. Cambridge Phil. Soc. **43**, 50 (1947).
[27]L.F. Richardson, Math. Gazette, **12**, 415 (1925).
[28]A. Ralston, Math. Comput. **16**, 431–437 (1962).
[29]J. Mazumder, Ph.D. thesis, London University (1978).
[30]R. Gordon and J. Cobonpue, Int. Heat Transfer Conf., Pt. II, 454–460 (1961).
[31]G.J. Davies, Ph.D. thesis, London University (1971).
[32]M. Eboo, Ph.D. thesis, London University (1979).
[33]J.M. Alexander (private communication).
[34]J. Mazumder, W.M. Steen, and D.R.F. West, Department of Metallurgy and Materials Science, Imperial College, London, MOD Progress Report, Nov. 1977 to April 1978, Agreement AT/12037/0177 XR.
[35]J. Mazumder and W.M. Steen, Proc. Laser '77 Conference, Munich 1977.
[36]W.M. Steen and M. Eboo, Metal Construction, Vol. II, No. 7, pp. 332–335, July 1979.
[37]N. Christensen, V. deL. Davies, and K. Gjermundsen, Br. Weld. J. **FEB**, 54–75 (1965).
[38]W.G. Alwang, L.A. Cavanaugh, and E. Sammartins, Br. Weld. J. Research Supplement, 110S, March (1969).
[39]Y. Arata and I. Miyamoto, Trans. JWRI **1**, 11–16 (1972).
[40]R. Guenot and J. Racinet, Br. Weld. J. **AUG**, 427–435 (1967).
[41]Lin Tung-Po. IBM J. Res. Dev. **11**, 527–536 (1967).
[42]R.A. Bunting and G. Cornfield, J. Heat Transfer **FEB**, 117 (1975).